IEEE Access
Multidisciplinary | Rapid Review | Open Access Journal

Received June 20, 2018, accepted July 28, 2018, date of publication August 6, 2018, date of current version September 7, 2018.

Digital Object Identifier 10.1109/ACCESS.2018.2863554

Advanced Energy Management of a Novel Independent Metering Meter-Out Control System: A Case Study of an Excavator

RUQI DING[1], JUNHUI ZHANG[2], AND BING XU[2]

[1]Key Laboratory of Conveyance and Equipment, Ministry of Education, East China Jiaotong University, Nanchang 330013, China
[2]State Key Laboratory of Fluid Power and Mechatronic Systems, Zhejiang University, Hangzhou 310027, China

Corresponding author: Junhui Zhang (benzjh@zju.edu.cn)

This work was supported in part by the National Natural Science Foundation of China under Grant 51705152 and Grant 91748210, in part by the NSFC-Zhejiang Joint Fund for the Integration of Industrialization and Informatization under Grant U1509204, and in part by the Natural Science Foundation of Jiangxi Province of China under Grant 20161BAB216133 and Grant 20161BAB206150.

ABSTRACT An independent metering (IM) system is a promising alternative to the conventional load-sensing (LS) system. However, the common meter-in control method has impeded further improvement in energy efficiency and investment costs. This paper presents a novel energy management algorithm that combines meter-out (MO) valve control with pressure/flow hybrid pump control. First, the energy-saving performance and dynamic characteristics are analyzed. Then, by designing a coordinate control between the pump and valves, the system has mode switching, MO flow/pressure control, flow distribution, anti-flow saturation, and electronic overload protection capabilities. Compared with the general IM control coupling with a LS system, the proposed method has fewer throttling losses, better dynamic control, and higher application adaptability. This study is applied to a hydraulic-mechanical coupling model of a 2-ton mini excavator to compare the proposed control system with an LS system. Typical continuous actions, such as digging and dumping, are conducted to analyze energy efficiency and controllability, and some special operating conditions, such as flow saturation and pressure/power overload, are also studied.

INDEX TERMS Electrohydraulic, energy efficiency, control design, independent metering (IM), meter-out control (MO), excavator.

I. INTRODUCTION

Electrohydraulic (EH) systems are widely used, especially for mobile machinery applications, due to their excellent power-to-weight ratio, wide dynamic range, and high bandwidth. Currently, mobile machinery is increasingly confronted with the challenge of rising energy costs and stringent emission regulations. Therefore, energy-saving hydraulic systems have attracted an increasing amount of interest in academic and industrial circles [1]–[3].

Figure 1 displays the energy loss distribution of a conventional excavator load-sensing (LS) system. The energy losses in pumps, pipes and valves exceed 50%. These losses in pumps and pipelines are almost always caused by leakage and friction from these components; therefore, it is not possible to lower them by improving the hydraulic control system. Most of the energy loss resides in the valves and consists of three aspects: high-pressure margin, throttling loss, and load differential. To decrease the energy loss in the valves, a promising alternative (when compared with conventional proportional directional valves), referred to as an independent metering valve (IMV), is presented.

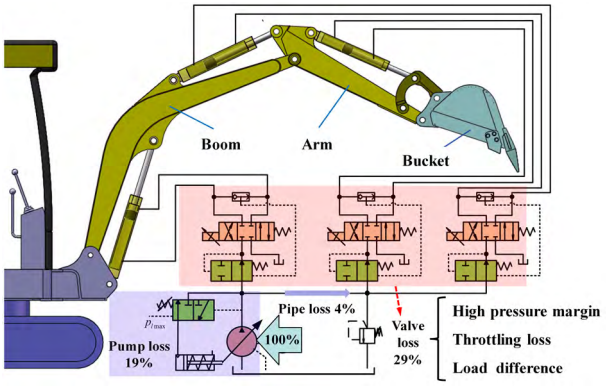

FIGURE 1. Energy consumption distributions of an excavator.

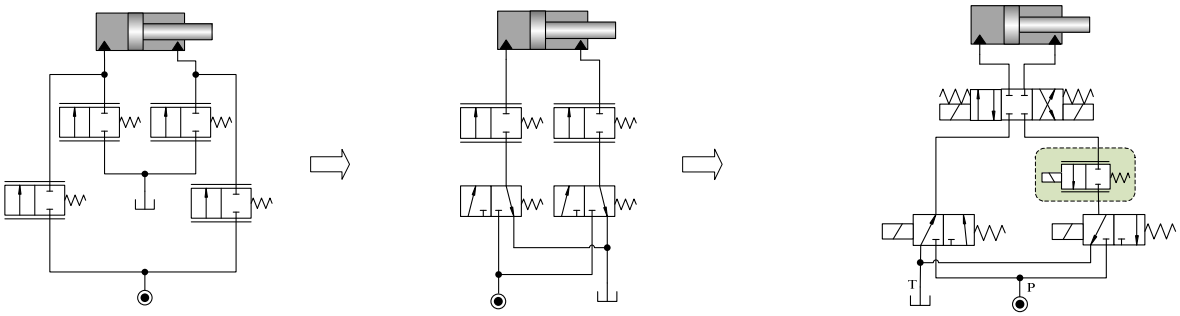

FIGURE 2. Optimizing IMV layout: (a) Common IMV layout, (b) Reducing the numbers of proportional valves with directional valves [9], (c) Simplifying IMV using single-edge meter-out control valve [10].

By introducing mechanically decoupled orifices at the cylinder chambers, the degrees of freedom (DOFs) of an IMV increase from 1 to 2. The additional DOF increases system efficiency, primarily by reducing the throttling losses in **Fig. 1** [4], [5]. However, one of the obstacles that prevents IM technology from wide use in industry is cost [6], [7]. The following suggestions have been made to overcome this challenge:

(1). Decrease the numbers of high-tech components;

(2). Eliminate the requirements for a complex EH control strategy; and

(3). Simplify the hardware layout.

Generally, four metering edges are mounted using IMVs because each port of the actuator may be charged or discharged by a supply and drain line, respectively [8]. However, only two metering edges must be controlled proportionally for a specific operation mode, while the others prepare for the next mode to change flow paths. Due to the high cost of proportionally controlled valves, some researchers have proposed novel valve arrangements consisting of two 2-way proportional valves combined with directional on/off valves [9], as shown in Fig. 2(b). Then, flow paths are changed only by the directional valves.

Although the numbers of proportional valves can be decreased, the circuit still includes both meter-in and meter-out edges. An interesting question is whether both edges are truly necessary. Vukovic and Murrenhoff further simplified the IMV using a meter-out control circuit in which the meter-in valve was no longer included, as shown in Fig. 2(c) [10]; compared with the classic IMV arrangement of four proportional valves shown in Fig. 2(a), only one proportional valve and three switching valves are required in this setup.

The simplest valve layout is a single-edge, meter-out control concept. This concept requires a novel control strategy to make full use of IM technology with only one proportional control valve. Therefore, the meter-out control method used in IM systems tends to attract more attention than hardware design does.

Hansen *et al.* [11] and Yao *et al.* [12] used a LS method of controlling pump pressure in a general IM system. However, this method impedes further improvement in energy efficiency by the high-pressure margin [13], as shown in **Fig. 1**. Therefore, Sitte proposed a meter-out control strategy [9]. Inspired by Sitte, Xu *et al.* presented a complete three-level controller with meter-out valve control and pump flow control [14]. Liu *et al.* presented pressure and flow accordance control for various excavator boom load conditions [15]. Jin *et al.* proposed combined robust velocity control and model-based pressure control algorithms to design an efficient pump and meter-out control for time-varying negative loads [16]. However, these researchers did not estimate this controller with continuous multiactuator action. In addition, other special conditions, including flow saturation nonlinearity and pressure/power overload, were not used in this control system. Considering these motivations, a systematic energy management algorithm with a meter-out control should be studied to meet the tougher requirements of energy efficiency.

Hydraulic excavators are widely used among today's vast array of heavy construction machinery, but their efficiency tends to be unsatisfactory [17], and these excavators are responsible for approximately 60% of the CO_2 emissions produced by construction machinery [18]. This work is performed using a 2-ton mini-excavator. Typical actions, including digging and dumping, are performed to compare the energy-saving and controllability performance to a conventional LS system.

II. METER-OUT CONTROL

Efforts have been made to research a complex coordination control structure, such that the metering areas of an IMV are associated with the pump displacement. Meter-in control is generally employed, which means that a meter-in valve is used to control the velocity and that the meter-out valve opens as much as possible to reduce pump pressure. Both pump pressure and flow control methods can be incorporated with meter-in control. In this case, throttling loss mainly occurs in the meter-in valve, which is referred to as the pressure margin p_m. However, the loss cannot be minimized since the meter-in spool is partly open.

TABLE 1. Comparisons of energy consumptions for different pump/valve coordinate control methods. (1—Saved energy due to the decreased pressure drops across meter-in valve; 2—Saved energy due to the maximum opening of meter-in valve).

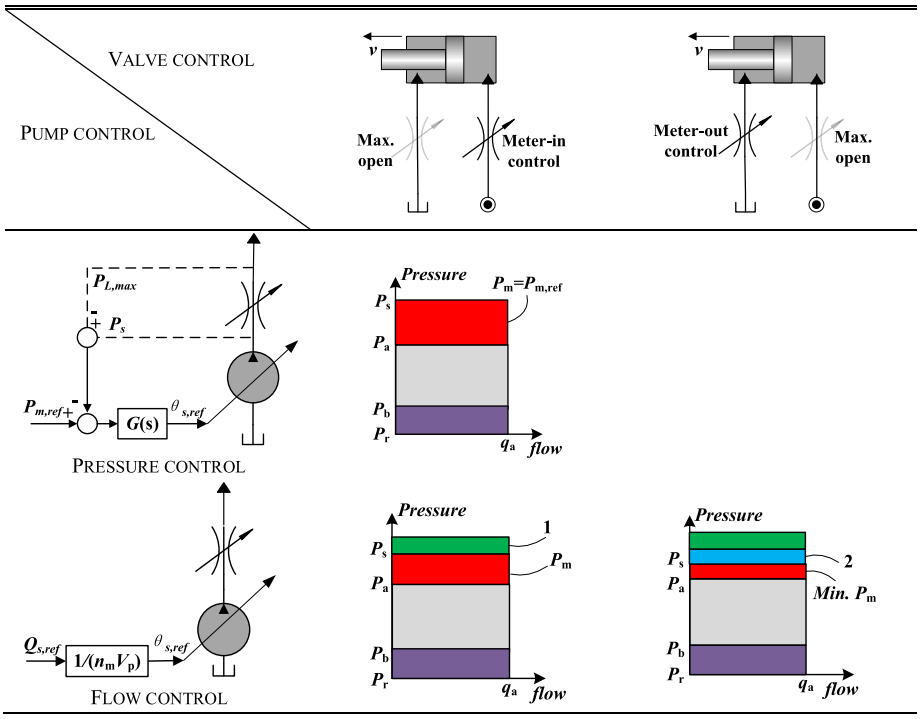

Meter-out control means that throttling losses shift from the meter-in side to the meter-out side. This measure has two main effects: the throttling losses across the meter-in valve decrease to optimize energy efficiency due to its maximum opening, and the hydraulic spring stiffness of the load increases significantly due to the increased pressure level. A comparison of energy consumption for each pump/valve coordinate control method is shown in Table 1. Note that meter-out control is only available for coupling with the pump flow control because, when pressure control is chosen, a sufficient pressure drop must be present to drive the desired flow rate across the meter-in orifice. Otherwise, the EH pressure compensation, used for velocity tracking and flow distribution, will not work.

System dynamics (except for energy efficiency) must also be studied because they influence the comfort of the excavator operator. Here, two control systems are compared: meter-in with pump pressure control (IM_LS; the most common system) and meter-out with pump flow control (IM_MO; the most efficient system).

1) CONVENTIONAL IM_LS SYSTEM

The dynamic behavior of this system can be described by (1)–(6).

Reference supply pressure:

$$p_{s,ref} = p_{m,ref} + p_a \tag{1}$$

Closed-loop pressure control:

$$k_p \cdot (p_{s,ref} - p_s) + k_i \cdot \frac{(p_{s,ref} - p_s)}{s} = \frac{q_s}{n_m} \tag{2}$$

Chamber pressure dynamic of the pump:

$$q_s - q_a = p_s \cdot C_p s \tag{3}$$

Flow rate across the meter-in valve:

$$q_a = K_{ca} \cdot (p_s - p_a) \tag{4}$$

Chamber pressure dynamic of the cylinder inlet:

$$q_a = A_a v + p_a \cdot \frac{V_a}{\beta_e} s \tag{5}$$

Cylinder movement equation:

$$m_t v s = p_a A_a - p_b A_b - B_p v - F_l \tag{6}$$

2) IM_MO SYSTEM

The swash control signal, considering the pump leakage:

$$q_s = \frac{\theta_{s,ref}}{\theta_{s,max}} n_m V_p - C_k p_s \tag{7}$$

Defining the dynamics of the pump as a first-order process with a time delay:

$$\frac{\theta_{s,ref}}{\theta_{s,max}} = \frac{K_p}{1 + T_p s} \cdot u_p \tag{8}$$

The equations for the IM_LS system are the same as (3)–(6).

Some simplifications are used to derive closed-loop transfer functions. The gain K_i is generally small enough to be ignored. A flow reference is mapped to a pump displacement to cancel out the flow nonlinearity caused by leakage coefficient C_k. Therefore, C_k can be omitted.

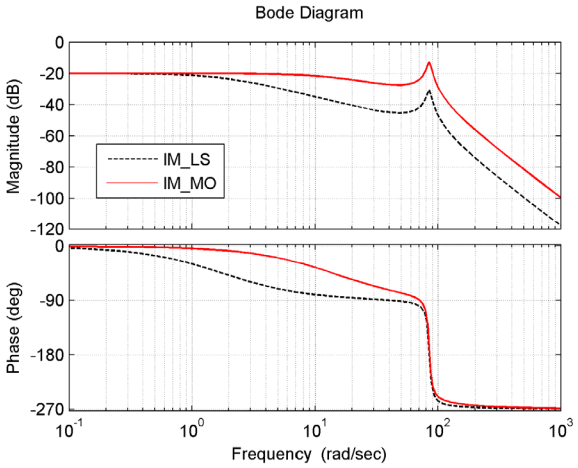

FIGURE 3. Bode diagrams of different hydraulic control system.

Additionally, outlet pressure p_b can be omitted because it is always controlled at a low level. Thus, the dynamic equations for the two systems are given by (9) and (10), respectively. The frequency domain is provided by the bode diagram in Fig. 6. Compared with the IM_LS system, the IM_MO system has higher bandwidth and lower damping, which means a faster response with more overshoot. Meanwhile, due to absence of feedback, the IM_MO system is still able to achieve higher stability.

$$\frac{v(s)}{p_{\mathrm{m,ref}}(s)} = \frac{K_i n_m V_p K_{ca} A_a}{a_3 s^3 + a_2 s^2 + a_1 s + a_0} \tag{9}$$

$$\frac{v(s)}{u_p(s)} = \frac{n_m V_p K_p A_a}{b_3 s^3 + b_2 s^2 + b_1 s + b_0} \tag{10}$$

$$\begin{cases} a_3 = m_t C_p K_{ca} \\ a_2 = m_t C_a K_i n_m V_p + B_p C_a K_{ca} \\ a_1 = B_p C_a K_i n_m V_p + A_a^2 K_{ca} \\ a_0 = A_a^2 K_i n_m V_p \end{cases} \quad \begin{cases} b_3 = m_t C_a T_p K_{ca} \\ b_2 = m_t C_a + B_p C_a T_p \\ b_1 = B_p C_a + A_a^2 T_p \\ b_0 = A_a^2 \end{cases} \tag{11}$$

III. ENERGY MANAGEMENT ARCHITECTURE

In respect to energy efficiency and controllability, IM_MO systems have prominent advantages. To take full advantage of a single-edge, meter-out control, including an improvement in energy efficiency and an extension of functionality, a multilevel energy management system is designed, as shown in **Fig. 4.**

The most significant feature of such a system is the multiple control modes for each level. The upper level conducts load control to achieve individual fluid paths, such as regeneration and recuperation [16], selects the most efficient operating mode in terms of the current system states and the desired motion trajectory, and controls the transitions between modes. The selected mode determines the distribution of the specific meter-out valve that enables significant energy savings without losing hydraulic circuit controllability

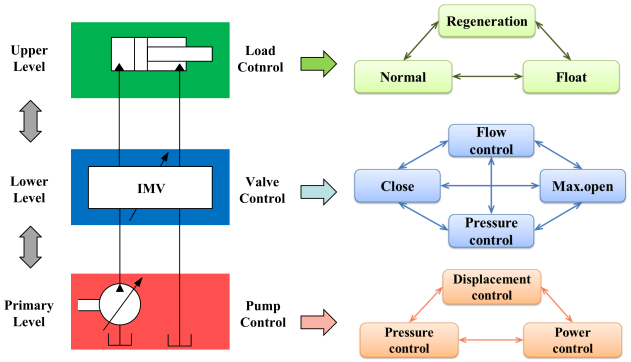

FIGURE 4. Energy management architecture.

for precise motion tracking. The lower level conducts valve control under the selected operating mode and primarily aims to achieve the desired motion characteristic and a secondary goal, such as throttling loss reduction. The primary level conducts pump control when incorporating an electronically controlled pump. Together with valve control, the primary level allows multiple target-variables to be controlled independently. The general variable combinations include cylinder velocity/pressure, position/pressure, and the pressures of the two ports.

A. LOAD CONTROL MODE

Operating modes can be subdivided into the following three categories according to the methods of flow supply [19], [20]:

1) NORMAL MODE (NOR.)

The flow is supplied by the pump, the meter-in chamber of the cylinder is connected to the pump, and the meter-out chamber is connected to the drain line.

2) REGENERATION MODE (REG.)

The cylinder is used as a transformer by connecting the cylinder chambers, thereby transforming a small load with a large flow into a heavy load with a small flow.

3) FLOAT MODE (FLO.)

With an overrunning load, both chambers are connected to the tank, and the load has a self-generated pressure that can be leveraged to cause flow.

According to the direction of both load force and velocity, load characteristics can be divided into four quadrants. Thus, operating modes using a single-edge, meter-out control valve are distributed as depicted in **Fig. 5**. On the basis of the defined modes, the target of the mode switch is to obtain the highest possible efficiency according to system state variables. **Table 2** analyzes the optimal mode switching logic in the dual-actuator system by considering energy efficiency.

B. VALVE CONTROL MODE

With the meter-out control approach, the flow or pressure of each actuator should be controlled only by the

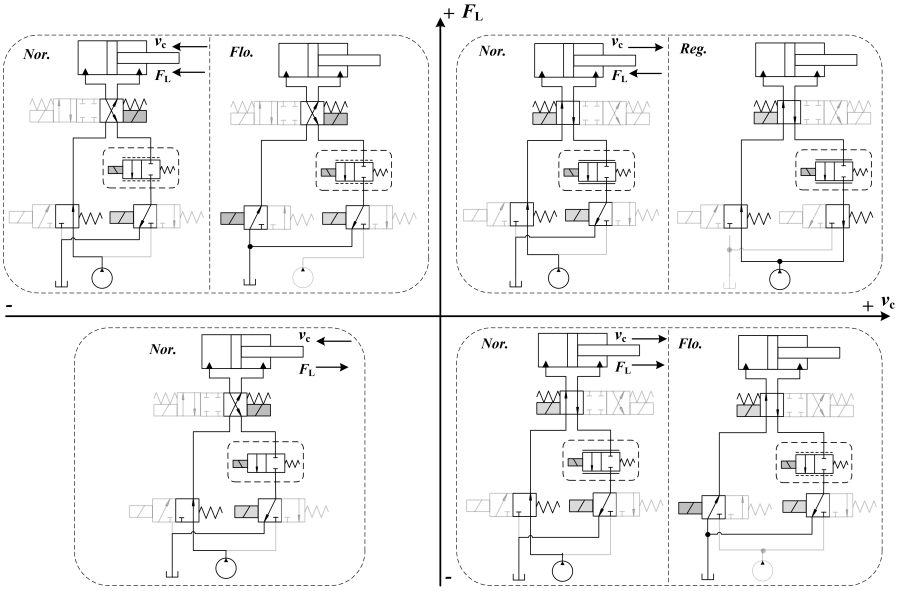

FIGURE 5. Operating modes covering four load quadrants (electromagnets filled with gray color are energized).

TABLE 2. Energy saving by mode switching.

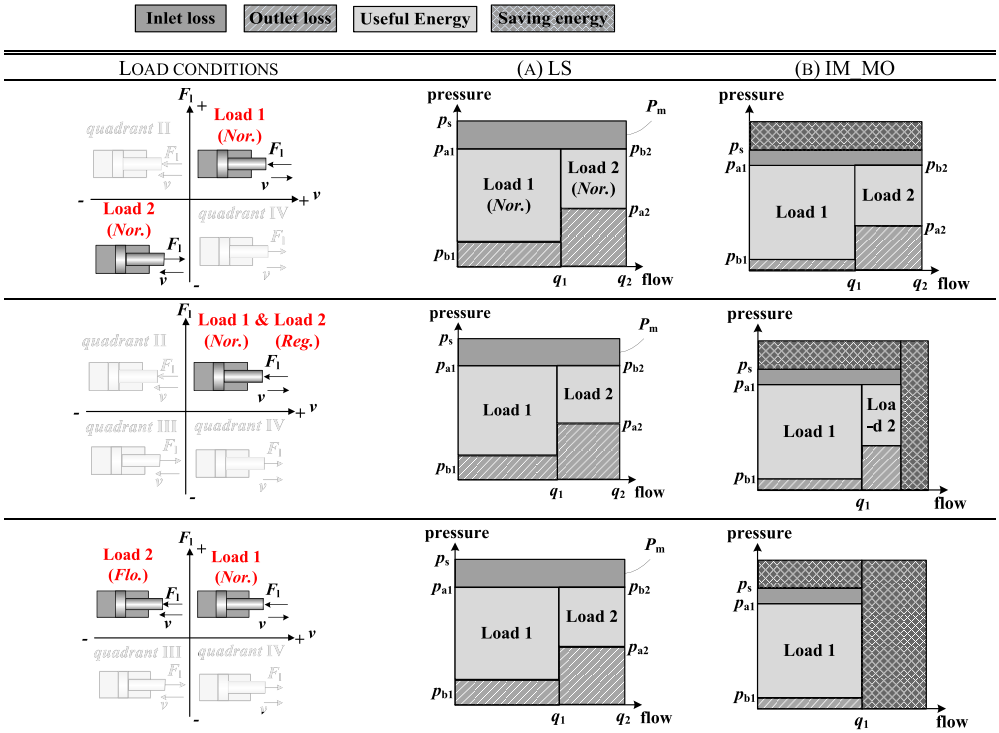

meter-out valve. Flow control is used to distribute the supply flow among multiple actuators. Nonlinearities and uncertainties exist between the flow and load pressure. Various adaptive control algorithms are recommended to solve the nonlinearity and uncertainty [21]–[24]; however, it is complex to design these adaptive control algorithms for excavator applications. In this paper, an electronic pressure compensator based on the inverse flow mapping of an orifice is used to cancel out the flow dependency of the load pressure, as depicted in **Fig. 6**. Meter-out pressure control is used to diminish the throttling losses across the meter-out valve and reduce the supply pressure. The pressure is generally adjusted

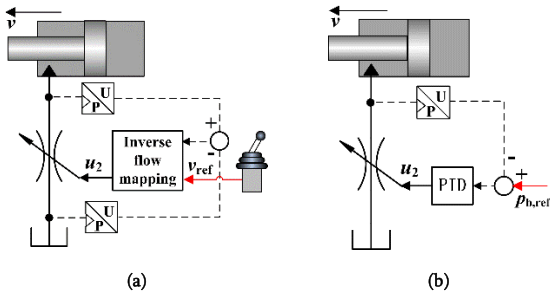

FIGURE 6. Schematic diagram of flow/pressure valve control: (a) meter-out flow control, (b) meter-out pressure control.

to 0.2 MPa to avoid cavitation due to a pressure feedback loop. The dead zone around the zero position is compensated by a cascade step unit equal to the dead-zone region.

C. PUMP CONTROL MODE

1) PRESSURE CONTROL

This method is a closed-loop control approach that improves upon conventional LS systems. This approach uses pressure transducers to replace the complex load-sensing hose and control the pump electronically, as shown in **Fig. 7**(a) [25]. Compared to those of conventional LS systems, the pressure losses in a directional valve can be reduced by optimizing the setting of the pressure margin p_m according to operating conditions. Despite this adjustment, p_m cannot be set perfectly due to the uncertainty in pressure drop in the hoses. Thus, unnecessary pressure losses still exist in the valve. In addition, closed-loop pressure control makes it possible for the system to still suffer from poor dynamic characteristics.

2) FLOW CONTROL

Flow control is used to remove the pressure feedback loop and control the pump electronically, according to the operator's command signals. The swash plate angle is then regulated according to the sum of all the requested load flows, as shown in **Fig. 7(b).** [26], [27]. This approach is an open-loop control method with two significant advantages: (1) the pressure drop between the pump and the load is given by the resistance of the hoses and valves, rather than a preset pressure margin $p_{m,ref}$; and (2) the stability problems associated with a closed-loop control method are eliminated [13]. Hence, it is possible to obtain higher efficiency and better dynamic characteristics than when using pressure control.

3) HYBRID CONTROL

Under most normal conditions, flow control is superior to pressure control, but there are still occasions that are difficult to handle using only flow control. One such occasion is a system overload. Using only flow control, the pump cannot drive the load when the required or actual power exceeds its maximal supply capability [28]. Another possible problem is over-matching the pump flow. If the flow delivered by the pump is higher than the sum of all the load flows, the pump pressure will increase until the system's main relief valve opens, turning the system into a constant pressure system and resulting in undesired energy losses. A flexible strategy to address these two problems is to merge flow control with pressure control, referred to as "hybrid flow/pressure/power control," as shown in **Fig. 7(c)**. A common hybrid solution is to design a switch strategy between the three control modes. If the load pressure or power measured surpasses the permissible value, the pump changes from flow control to pressure control to achieve overload protection. This switch is also suitable to address flow over-matching by measuring the pressure difference between the pump and load instead of the load pressure. However, this discrete switching, in terms of the measured pressure, always has a discontinuity problem, which requires a special switching strategy to avoid a pressure impact or oscillation [29], [30].

IV. DETAILED COORDINATE CONTROL OF THE THREE LEVELS

According to the demonstrations of each individual level controller, there are several problems associated with using a coupling meter-out valve control. The problems should be addressed using coordinate control of the three levels.

(1) Under some special conditions, such as an overload, the pump is unable to supply sufficient power or pressure using only flow control, as depicted in **Fig. 8**. In this case,

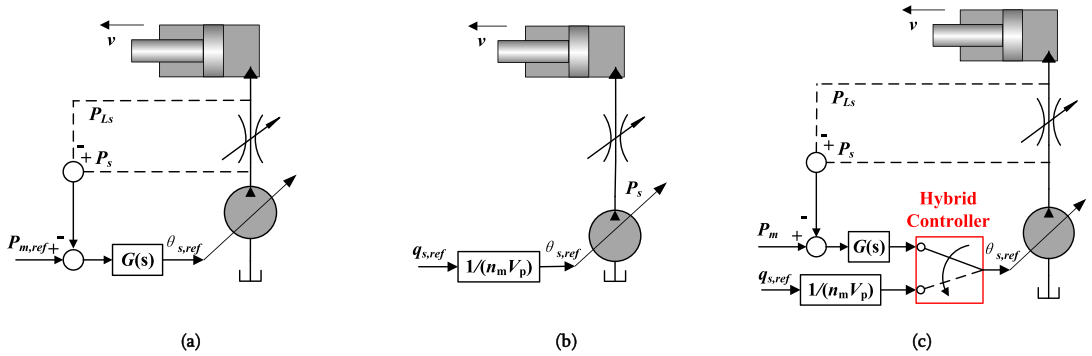

FIGURE 7. Schematic diagram of pump control methods: (a) Pressure control, (b) Flow control, (c) Hybrid control.

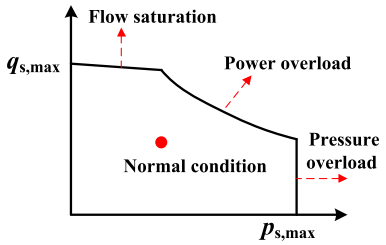

FIGURE 8. Possible pump operating conditions.

the pump should guarantee the required supply pressure and simultaneously downscale the supply flow to continue the motions. This compensation requires a switch from flow control to pressure control.

(2) The valves hold the load when there is no command signal. In this state, the pump should maintain a relatively low standby pressure to minimize the viscous drag losses. This standby pressure is much less than the load pressure. Whenever the actuation is commanded to move, the load would drop at first due to the absence of the meter-in valve.

(3) Both the meter-in and meter-out orifices contain four states: closed, flow control, pressure control and fully opened. The configurations of their functions depend on not only the load characteristics but also the operating modes of the loads. Therefore, valve control selection is critical for distributing system flow and decreasing system pressure or flow simultaneously in a multiactuator system.

A. PUMP HYBRID CONTROL

When the system pressure or power is under the allowable scope, the flow controller is employed to adjust the pump swash-plate angle in an open-loop way. The controller receives flow references from all joysticks and uses a feed-forward method to determine the swash-plate angle. This feed-forward block uses a map from the pump flow to the swash-plate angle by applying (12), which maps the flow to the pump pressure and the rotator speed. This arrangement can consequently cancel out the nonlinear dependency of the pump pressure.

$$\frac{\theta_{s,ref}}{\theta_{s,max}} = \frac{(\sum q_{i,ref} + p_s \cdot C_k)}{V_p n_m} \tag{12}$$

Protection against pressure and power overloads is implemented by adding pressure control to the flow controller. The system takes the allowable scope $p_{s,max}$ or P_{max} as its reference and uses a proportional-integral controller to downscale the pump flow by a negative flow reference q. As a consequence, the pump supply pressure is guaranteed to continue the required movement. Thus, the reference velocity of each actuator decreases proportionally by adjusting their respective valve openings due to the diminishing pump flow reference, which is identical to flow saturation control.

The pressure control is only activated when the actual pump pressure or power is larger than the upper limit of the supply. The switch depends on dynamical pump pressure. Therefore, the switch may encounter instability, which drastically degrades control performance. The average dwell time can be used to solve this issue [31]. In this study, dwell time t_p is set to determine the interval between two consecutive switching actions; a switching action can happen only at the end of a windowing period. The complete architecture of the pump control is shown in **Fig. 9**. Concerns regarding flow saturation are introduced in later sections.

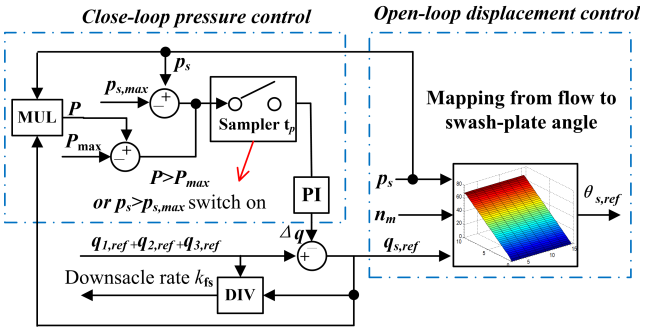

FIGURE 9. Schematic diagram of pump hybrid control.

B. TIMING CONTROL OF VALVES AND PUMP

To overcome the second aforementioned problem, the operation time between the pump and valve should be strictly controlled. The pump pressure must meet the load pressure prior to opening the load holding valves. Otherwise, large

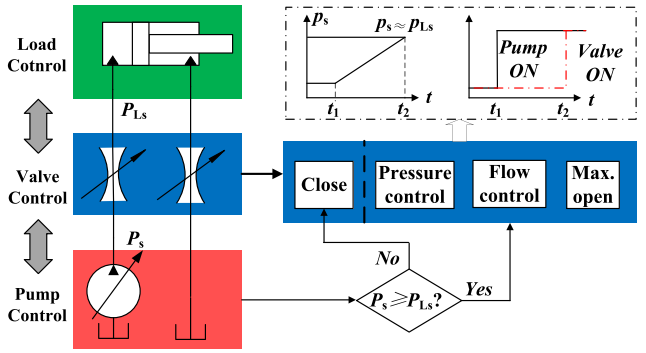

FIGURE 10. Timing control of the valves and pump.

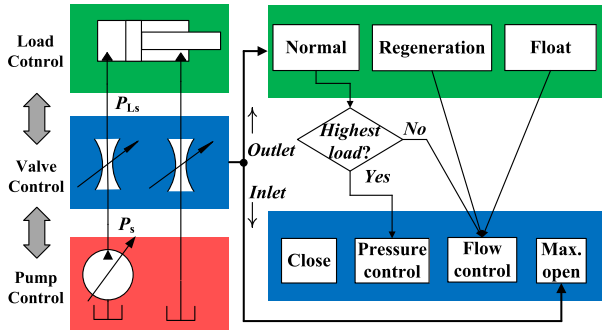

FIGURE 11. Configuration of valve control functions.

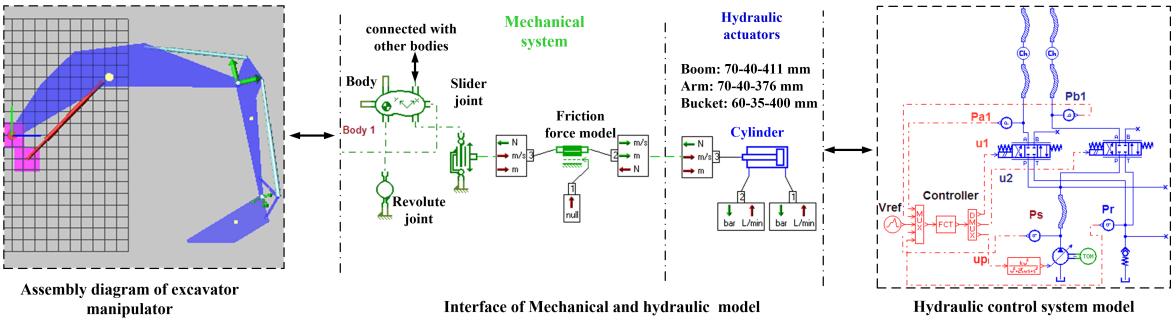

FIGURE 12. Hydraulic-mechanical coupling simulation model of excavator.

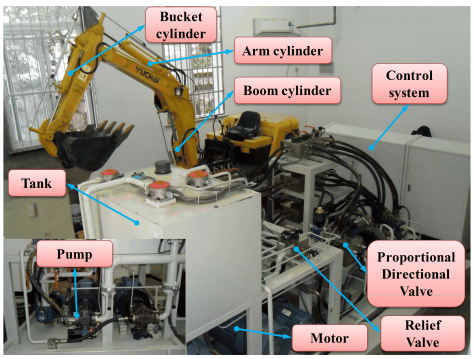

FIGURE 13. Test rig of IM_MO control system.

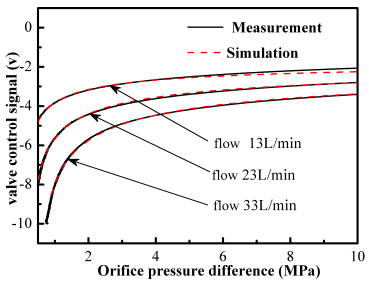

FIGURE 14. Comparison of the measured and simulated valve flow mapping.

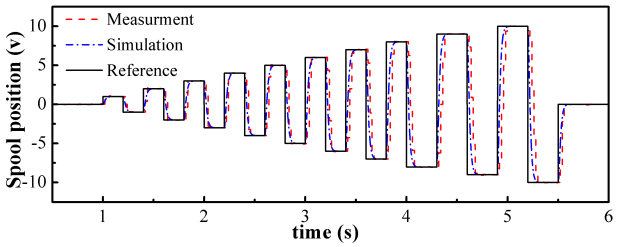

FIGURE 15. Comparison of the measured and simulated valve response.

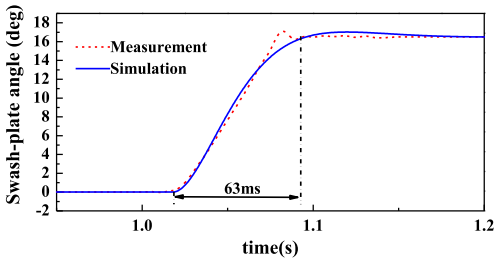

FIGURE 16. Comparison of the measured and simulated pump response.

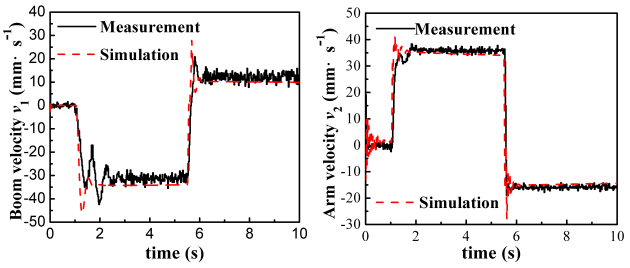

FIGURE 17. Comparison of the measured and simulated specific movements.

pressure peaks and a decline in velocity will occur. For this reason, the pump pressure increases to the load pressure by a preset displacement command. The valves will not open until the pump pressure first equals to the load pressure. The logic between the pump and valves is shown in **Fig. 10**.

C. CONFIGURATION OF THE VALVE CONTROL MODE

After pump matching, the valve starts to open to control the motion of the actuators. The flow chart listed below in **Fig. 11** configures the valve control to distribute the flow and reduce the system pressure in the multiactuator system.

First, it is decided whether there are actuators operating in regeneration mode or float mode. In float mode, the pump is not required to supply flow due to the overrunning load. The valve on the high-pressure side always controls the flow, and the valve in the low-pressure side opens fully to save energy. Therefore, meter-out flow control is chosen. In regeneration mode, the valve control also selects meter-out flow control by considering system damping. Cylinder drive damping increases because hydraulic spring stiffness increases significantly due to the higher pressure [9].

Second, among the actuators in normal mode, the controller decides which actuator operates with the highest load. For the highest load, meter-out pressure control is chosen to keep the pressure drop in the drain line. It is beneficial to

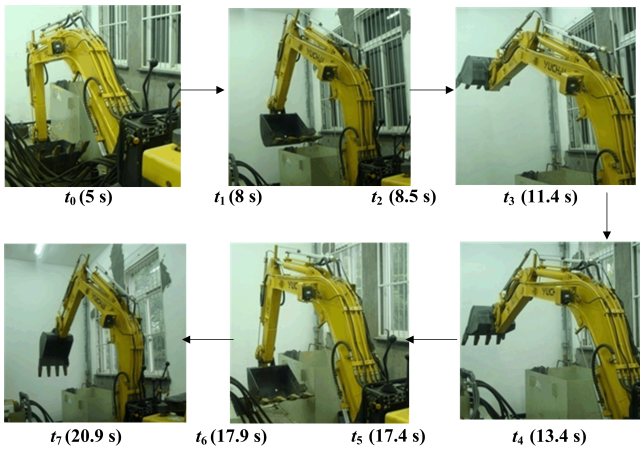

FIGURE 18. Typical action including digging and dumping soils.

avoid cavitation while keeping the supply pressure as low as possible to save energy.

Finally, for each actuator with a low load, meter-out flow control is selected to control actuator flow. The pressure level is raised to the supply pressure due to the absence of meter-in throttling. The meter-out valve acts as the flow distributor. Then, the flow of the highest load is given by (13):

$$q_{\text{high}} = q_{\text{s}} - \sum q_{i,\text{low}} \tag{13}$$

If the sum of the flows from all the loads exceeds the maximum flow of the pump, the flow saturation controller is activated such that the flow of each actuator proportionally decreases according to a scaled-down ratio k_{fs}. The ratio k_{fs} is estimated in terms of the pump flow as:

$$k_{fs} = \frac{q_{\text{s,max}}}{\sum q_{\text{i,ref}}} \tag{14}$$

Then, the flows of the actuators using meter-out flow control must be decreased via (15). This decrease is achieved by diminishing the opening areas of the meter-out valves accordingly. The flow of the highest load is also determined by (13).

$$q_{2,\text{fs}} = k_{fs} \cdot q_{2,\text{ref}} \quad q_{3,\text{fs}} = k_{fs} \cdot q_{3,\text{ref}} \tag{15}$$

V. APPLICATION ON AN EXCAVATOR

A. MODELING A 2-TON EXCAVATOR USING IM CONTROL

The proposed energy management algorithm is applied in a hydraulic-mechanical coupling simulation model. The planar block is used to model the manipulators of the excavator, and the hydraulic block is used to model the IM system. The interface between the two parts is exhibited in **Fig. 12**, and the parameters of three actuators are listed in the hydraulic actuator part. This coupling model has been calibrated and verified using a test rig, as shown in **Fig. 13.**

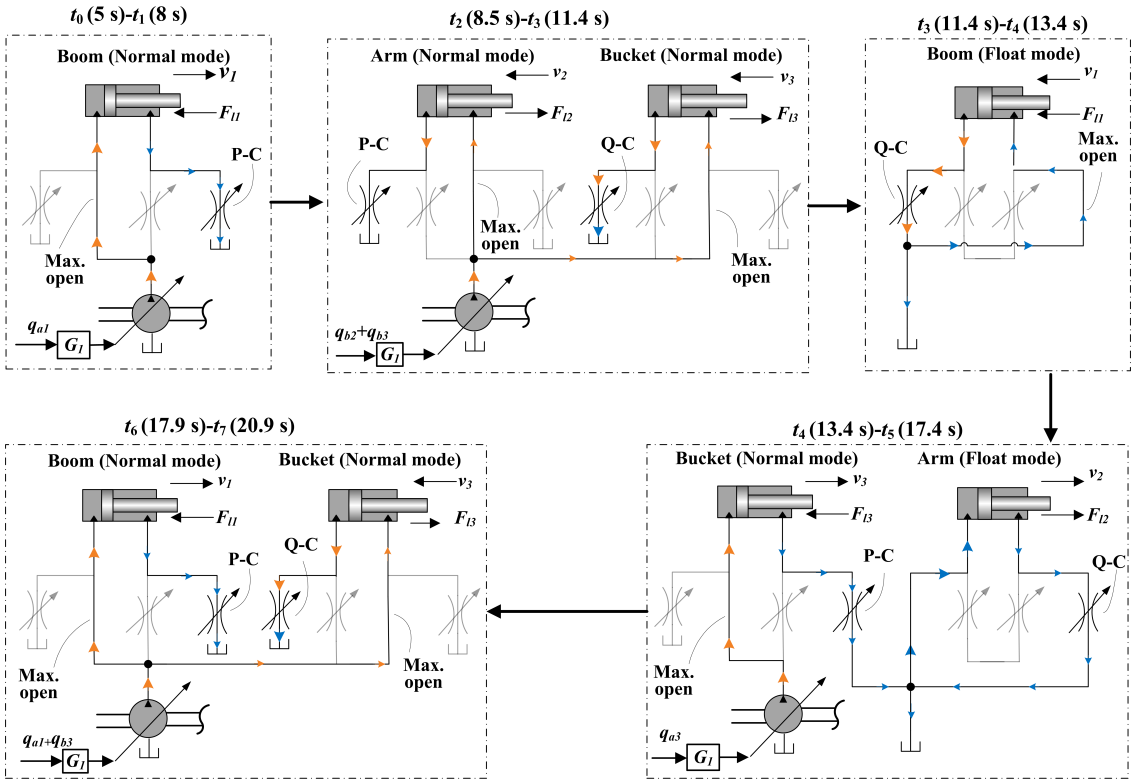

FIGURE 19. The valve and pump control configurations for the typical action cycle.

I. Verification of static characteristics: valve flow versus pressure differences based on the nonlinear model of the orifice equation, as shown in **Fig. 14**.

II. Verification of the dynamic characteristics of the components: step responses of the valves (**Fig. 15**) and pump (**Fig. 16**) for which a group of step voltage inputs, ranging from 1 V to 10 V, are applied to an electromagnet with a spool in oil and a pump pressure of zero.

III. Verification of a typical boom and arm with alternate motions, as shown in **Fig. 17**:

(1) The boom first lowers and then lifts. The valve control signals are ±2 V;

(2) The arm first retracts and then extends. The valve control signals are ±4 V.

Verifications by the test rig prove that the method has the capability to capture system dynamics and static characteristics accurately. Therefore, it can be used to simulate the complete typical action cycle of this excavator.

B. VERIFICATION WITH A TYPICAL ACTION CYCLE

A group of continuous actions, including digging and dumping, are simulated to analyze the proposed controller, as shown in **Fig. 18**. Comparisons are conducted between the IM_MO and conventional LS systems, of which the preset pressure margin $p_{m,ref}$ is 1.6 MPa. The control methods used for various operating times are depicted in **Fig. 19**, where:

P-C: meter-out pressure control

Q-C: meter-out flow control

With the IM_MO system, the time sequence of the entire movement can be described as:

(1) t_0(5 s) - t_1(8 s): The boom lifts and other actuators are stationary. The boom is operated in normal mode due to the resistive load. Thus, the meter-out valve controls the backpressure to a low level (0.2 MPa) to reduce the supply pressure.

(2) t_1(8 s) - t_2(8.5 s): All the actuators are stationary.

(3) t_2(8.5 s) - t_3(11.4 s): Both the arm and bucket extend, and the boom is stationary. The two actuators work simultaneously under the resistive loads, of which the arm cylinder has the highest load. Therefore, the meter-out valve of the bucket controls its flow to track the reference velocity, and the meter-out valve of the arm controls its backpressure. The velocity of the arm is determined by the difference between the supply flow and the bucket flow.

(4) t_3(11.4 s) - t_4(13.4 s): The boom is lowered, and the other actuators are stationary. The boom is operated in float mode without any supply from the pump due to a sufficient overrunning load, and the meter-out valve controls the flow out of its head-side chamber.

(5) t_4(13.4 s) - t_5(17.4 s): Both the arm and bucket retract to dig soil, and the boom is stationary. Due to the sufficient overrunning load, the arm is operated in float mode, and only the bucket requires supply from the pump. Therefore, the meter-out valve of the arm controls its flow to track the reference velocity, and the meter-out valve of the bucket controls its backpressure.

(6) t_5(17.4 s) - t_6(17.9 s): All actuators are stationary.

(7) t_6(17.9 s) - t_7(20.9 s): Both the boom and bucket lift to dump soil, and the arm is stationary. The two actuators work simultaneously under resistive loads, of which the boom cylinder has the higher load. Therefore, the meter-out valve of the bucket controls its flow, and the meter-out valve of the boom controls its backpressure. The velocity of the boom is determined by the difference between supply flow and bucket flow.

1) CHARACTERISTICS ANALYSIS

First, motion control performance is analyzed. Comparisons pertaining to velocity dynamics are exhibited in **Fig. 20**. When the actuators are supplied by the pump [normal mode (Nor.)], the oscillations with IM_MO are less than those of the LS system. The results verify that better stability can be obtained with the IM_MO system. However, the response time of IM_MO system is still slightly faster. The higher overshoots of the LS system may be caused by the transient

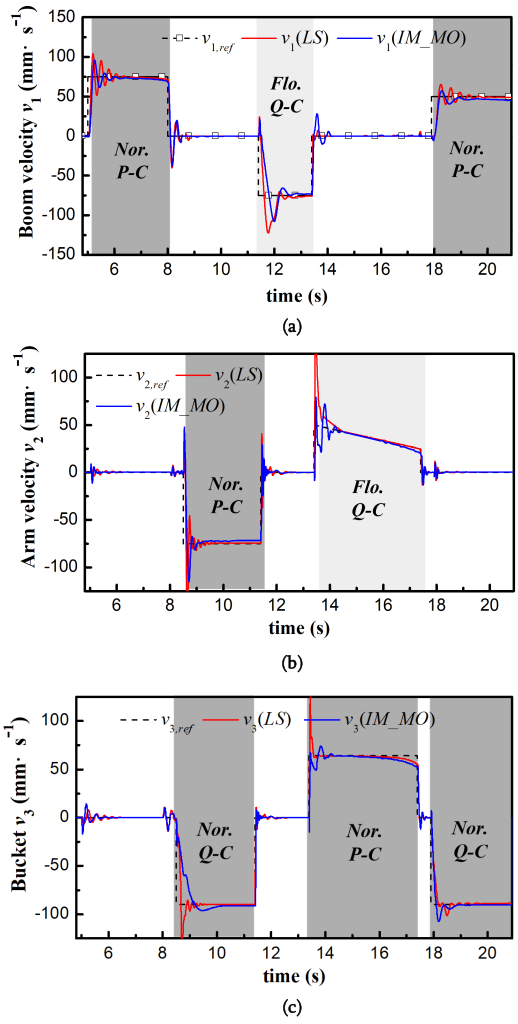

FIGURE 20. Actuator velocities during typical action cycle: (a) Boom velocity, (b) Arm velocity, (c) Bucket velocity.

impact of the closed-loop pressure controller of the pump. In the IM_MO system, the pump is steered with an open-loop controller. Therefore, there is less of an impact on the pump supply, which is depicted by the comparison of supply flows in **Fig. 21(b)**. When the actuators are driven by the overrunning loads [Float mode (Flo.)], higher stability is attained with IM_MO. However, sometimes a slower response occurs because, in this case, the driven pressure provided by the overrunning load is very low.

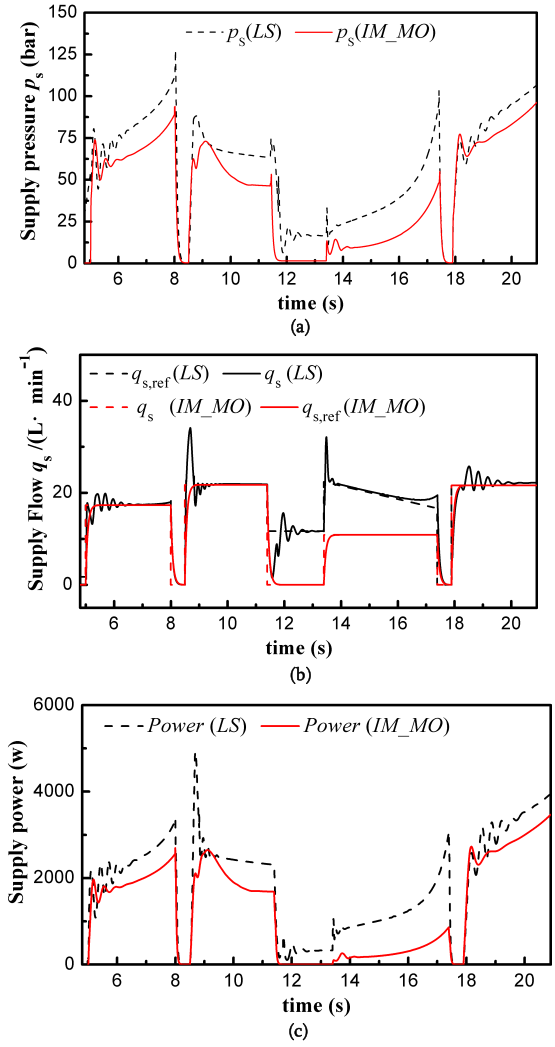

FIGURE 21. Pump supply during typical action cycle: (a) Supply pressure, (b) Supply flow, (c) Supply power.

Next, the energy-saving performance is analyzed. In normal mode, the inlet pressure losses of IM_MO decrease due to the full opening of the meter-in valve, and the outlet pressure losses of IM_MO are also smaller than those of the conventional LS system because the meter-out valve can be independently regulated to a large opening. This can be seen in the comparison of boom cylinder pressures in **Fig. 22** when the time ranges from [5 s, 8 s] to [17.9 s, 20.9 s]. The cylinder pressures for the arm and bucket are the same as those of the boom in normal mode; therefore, their curves are

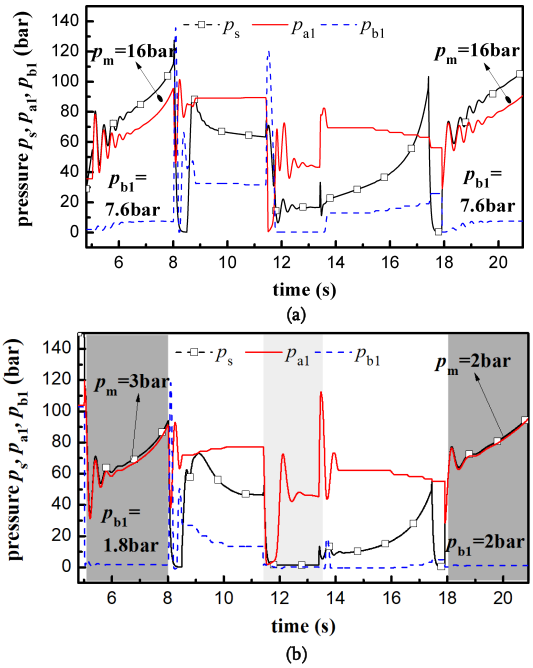

FIGURE 22. Pressures of boom cylinder: (a) LS system, (b) IM_MO system.

omitted here. The decrease in both the inlet and outlet losses contributes to the reduction in the supply pressure, as shown in **Fig. 21(a)**. In float mode, supply flow decreases because the actuator with an overrunning load does not demand any supply flow. This can be seen in the supply flow comparison in **Fig. 21(b)** from 11.4 s to 17.4 s when the boom and arm are driven by their potential loads. The hydraulic power pertaining to the complete movement cycle is described in **Fig. 21(c)**. With the decrease in supply pressures and flows, the integral of the supply power from t_0 to t_7 indicates that the energy-saving rate using IM_MO is up to 28%.

C. VERIFICATION OF FLOW SATURATION

The simulation results under flow saturation are shown in **Fig. 23**, which assumes that the maximum supply flow is 34.5 L/min. When flow saturation begins ($t = 7.1$ s), the boom velocity first decreases, and the other actuators are seldom affected due to the flows entering the low-load actuators, which is undesirable for a multiactuator system. Using the proposed algorithm, the areas of the meter-out valves diminish synchronously such that the velocities of the three actuators decrease proportionally according to the scale-down ratio k_{fs}.

D. VERIFICATION OF THE OVERLOAD CONDITION

Assuming that the maximum supply pressure is 9 MPa, overload protection starts by transferring the pump from flow control to pressure control, as the simulation results show in **Fig. 24**. The supply pressure is maintained below 9 MPa by decreasing the velocities of the three actuators proportionally. Although more time is required to track a motion trajectory,

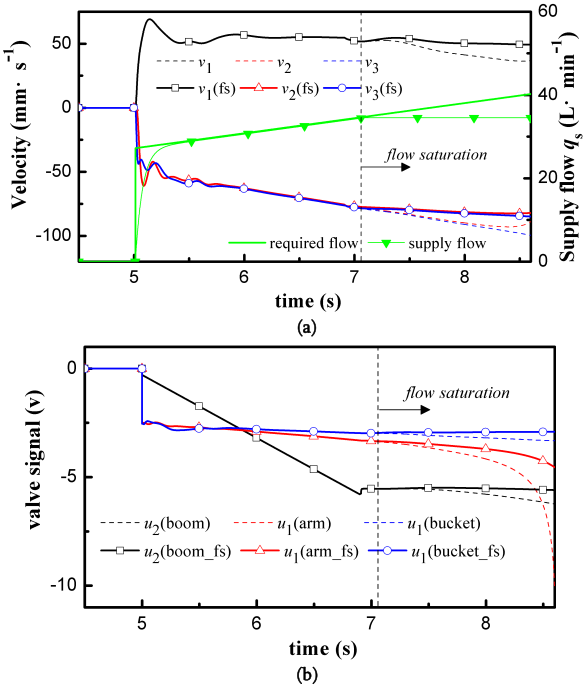

FIGURE 23. Simulations of flow saturation control: (a) Velocities and flow, (b) Meter-out valve control signals.

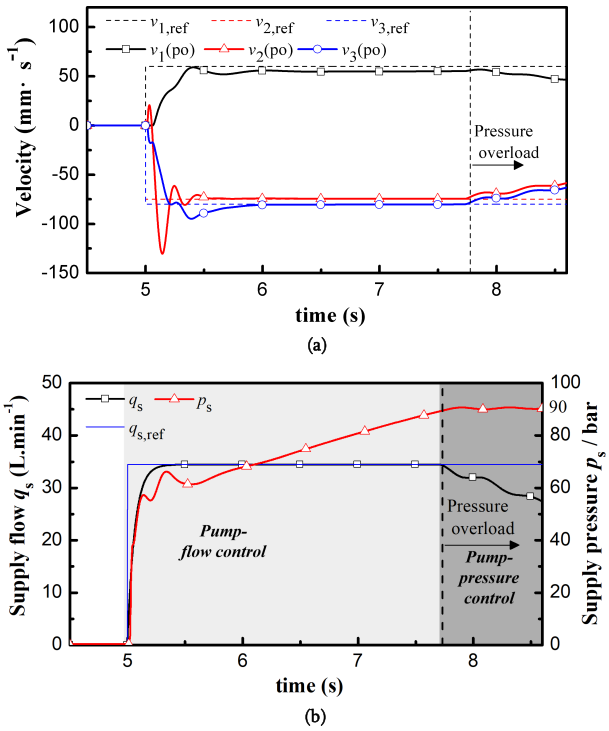

FIGURE 24. Simulations of pressure overload control: (a) Velocities, (b) Supply flow and pressure.

the machinery is able to continue operating with higher reliability and safety. The proposed algorithm also has an effect on the power overload condition. In **Fig. 25,** the supply power is maintained at no more than its upper limit (4.5 kW) in the same way as the pressure overload protection.

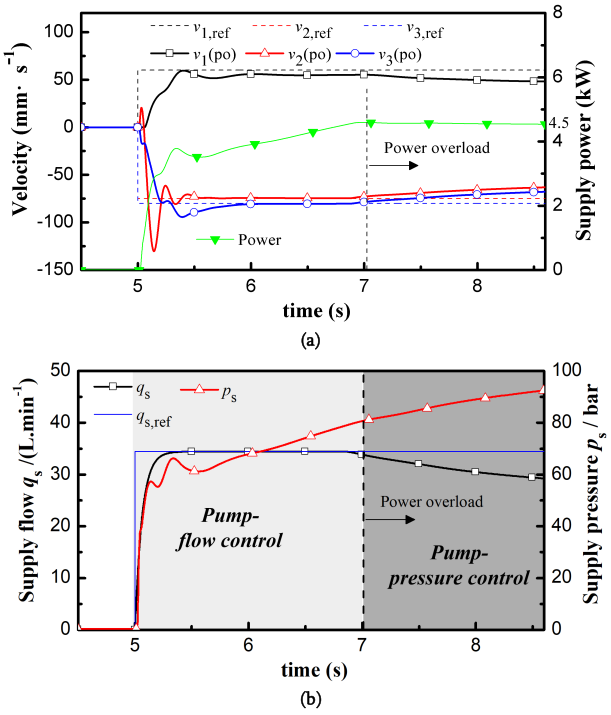

FIGURE 25. Simulations of power overload control: (a) Velocities and power, (b) Supply flow and pressure.

VI. CONCLUSION

This paper presents an advanced energy management algorithm for an independent metering meter-out control system for mobile machinery. The proposed algorithm contains three DOFs for the control: the individual inlet and outlet orifices and pump displacement. By associating meter-out valve control with pump flow/pressure hybrid control, the inlet orifice always opens maximally to minimize pressure loss across the valve. Based on this approach, a three-level energy management system is designed to electronically achieve primary functions, including motion characteristic tracking and saving energy as well as auxiliary functions, including anti-flow saturation and overload protection.

Continuous digging and dumping actions are verified using a hydraulic-mechanical coupling model with a 2-ton mini-excavator. The results demonstrate that, by using the proposed algorithm, better controllability can be obtained with higher stability and faster responses than that with a LS system. The energy savings rate for a complete action cycle can reach 28% compared with a LS system. Auxiliary functions, such as anti-flow saturation and overload protection, are also effective to continue the desired movement under extreme operating conditions.

APPENDIX

NOMENCLATURE

A_a	Head side area of cylinder [m^2]
A_b	Rod side area of cylinder [m^2]
B_c	Viscous friction coefficient [N/(m · s^{-1})]
C_p	Coefficient of pump pressure chamber [1]

C_k	Leakage coefficient [1]
F_f	Friction force [N]
F_l	Load force [N]
K_{ca}	Flow-pressure coefficient of meter-in valve [1]
k_{fs}	Scale factor of flow saturation [1]
K_i	Integration coefficient [1]
K_p	Proportion coefficient [1]
m_t	Load mass [kg]
n_m	Rotational speed of pump [r/min]
P	Hydraulic power [W]
P_{max}	Hydraulic power limit [W]
p_a	Pressure in head side chamber [Pa]
p_b	Pressure in rod side chamber [Pa]
p_{Ls}	Load pressure [Pa]
p_m	Pressure margin between pump and load [Pa]
$p_{m,ref}$	Preset pressure margin between pump and load [Pa]
p_r	Drain pressure [Pa]
p_s	Pump pressure [Pa]
$p_{s,max}$	Pump pressure limit [Pa]
$p_{s,ref}$	Reference Pump pressure [Pa]
q_{high}	Flow for the actuators with the highest load [m^3/s]
$q_{i,fs}$	Reference flow for different actuators by anti-flow saturation, i = 1 for boom, i = 1 for boom, i = 2 for arm, i = 3 for bucket [m^3/s]
$q_{i,ref}$	Reference flow for different actuators, i = 1 for boom, i = 1 for boom, i = 2 for arm, i = 3 for bucket [m^3/s]
$q_{i,low}$	Flow for different actuators with low load ([m^3/s]
q_s	Pump flow [m^3/s]
$q_{s,ref}$	Reference flow for pump [m^3/s]
u_1	Control voltage of valve 1 [v]
u_2	Control voltage of valve 2 [v]
u_p	Control voltage of pump [v]
t_0	Starting time for a task [s]
t_i	End time for a task, i = 1, 2, 3, … [s]
v_a	Chamber volume of cylinder head side [m^3/r]
V_p	Pump displacement [m^3/r]
v	Actuator velocity [m/s]
v_i	Cylinder velocity, i = 1 for boom, i = 2 for arm, i = 3 for bucket (m/s) [m/s]
β_e	Oil elasticity modulus [Pa]
$\theta_{s,ref}$	Reference angle of pump swash plate [rad]
$\theta_{s,max}$	Max. angle of pump swash plate [rad]

REFERENCES

[1] W. Shen, H. Huang, Y. Pang, and X. Su, "Review of the energy saving hydraulic system based on common pressure rail," *IEEE Access*, vol. 5, pp. 655–669, 2017.

[2] W. Wu and C. Yu, "Simulation and experimental analysis of hydraulic directional control for displacement controlled system," *IEEE Access*, vol. 6, pp. 27993–28000, 2017.

[3] C. Liu, Y. Liu, J. Liu, G. Yang, X. Zhao, and W. Quan, "Electro-hydraulic servo plate-inclined plunger hydraulic transformer," *IEEE Access*, vol. 4, pp. 8608–8616, 2016.

[4] J.-C. Lee, K.-C. Jin, Y.-M. Kwon, L.-G. Choi, J.-Y. Choi, and B.-K. Lee, "Development of the independent metering valve control system and analysis of its performance for an excavator," presented at the FPMC, Bath, U.K., 2016.

[5] R. Ding, B. Xu, J. Zhang, and M. Cheng, "Self-tuning pressure-feedback control by pole placement for vibration reduction of excavator with independent metering fluid power system," *Mech. Syst. Signal Process.*, vol. 92, pp. 86–106, Aug. 2017.

[6] H. Murrenhoff and S. S. Milos, "An overview of energy saving architectures for mobile applications," presented at the 9th Int. Conf. Fluid Power, Archen, Germany, Mar. 2014.

[7] J. Lübber, A. Sitte, and J. Weber, "Pressure compensator control—A novel independent metering architecture," presented at the 10th Int. Conf. Fluid Power, Dresden, Germany, 2016.

[8] K. Choi, J. Seo, Y. Nam, and K. U. Kim, "Energy-saving in excavators with application of independent metering valve," *J. Mech. Sci. Technol.*, vol. 29, no. 1, pp. 387–395, 2015.

[9] A. Sitte, "Structural design of independent metering control systems," presented at the 9th Int. Conf. Fluid Power, Archen, Germany, 2014.

[10] M. Vukovic and H. Murrenhoff, "Single edge meter out control for mobile machinery," presented at the FPMC, Bath, U.K., 2014.

[11] A. H. Hansen, H. C. Pedersen, L. Wachmann, and T. O. Andersen, "Design of energy efficient SMISMO-ELS control strategies," in *Proc. 6th Int. Conf. Fluid Power Mechatronics*, Beijing, China, 2011, pp. 522–527.

[12] J. Yao, B. Li, X. Kong, and F. Zhou, "Displacement and dual-pressure compound control for fast forging hydraulic system," *J. Mech. Sci. Technol.*, vol. 30, no. 1, pp. 353–363, 2016.

[13] M. Axin, B. Eriksson, and P. Krus, "Flow versus pressure control of pumps in mobile hydraulic systems," *Proc. Inst. Mech. Eng. I, J. Syst. Control Eng.*, vol. 228, no. 4, pp. 245–256, 2014.

[14] B. Xu, R. Ding, J. Zhang, M. Cheng, and T. Sun, "Pump/valves coordinate control of the independent metering system for mobile machinery," *Automat. Construct.*, vol. 57, pp. 98–111, Sep. 2015.

[15] B. Liu, L. Quan, and L. Ge, "Research on the performance of hydraulic excavator boom based pressure and flow accordance control with independent metering circuit," *Proc. Inst. Mech. Eng. E, J. Process Mech. Eng.*, vol. 231, no. 5, pp. 901–913, 2017.

[16] J. Mengren and W. Qingfeng, "Efficient pump and meter-out control for electrohydraulic system with time-varying negative load," *Proc. Inst. Mech. Eng. I, J. Syst. Control Eng.*, May 2018, doi: 10.1177/0959651818776868.

[17] Q. Chen, T. Lin, and H. Ren, "A novel control strategy for an interior permanent magnet synchronous machine of a hybrid hydraulic excavator," *IEEE Access*, vol. 6, pp. 3685–3693, 2018.

[18] M. Vukovic, R. Leifeld, and H. Murrenhoff, "Reducing fuel consumption in hydraulic excavators—A comprehensive analysis," *Energies*, vol. 10, no. 5, p. 687, 2017.

[19] R. Ding, B. Xu, J. Zhang, and M. Cheng, "Bumpless mode switch of independent metering fluid power system for mobile machinery," *Automat. Construct.*, vol. 68, pp. 52–64, Aug. 2016.

[20] B. Eriksson, "Mobile fluid power systems design: With a focus on energy efficiency," Ph.D. dissertation, Dept. Manage. Eng., Linköping Univ., Linköping, Sweden, 2010.

[21] Z. Chen, B. Yao, and Q. Wang, "Accurate motion control of linear motors with adaptive robust compensation of nonlinear electromagnetic field effect," *IEEE/ASME Trans. Mechatronics*, vol. 18, no. 3, pp. 1122–1129, Jun. 2013.

[22] X. Zhao, P. Shi, and X. Zheng, "Fuzzy adaptive control design and discretization for a class of nonlinear uncertain systems," *IEEE Trans. Cybern.*, vol. 46, no. 6, pp. 1476–1483, Jun. 2016.

[23] H. Wang, P. X. Liu, and P. Shi, "Observer-based fuzzy adaptive output-feedback control of stochastic nonlinear multiple time-delay systems," *IEEE Trans. Cybern.*, vol. 47, no. 9, pp. 2568–2578, Sep. 2017.

[24] H. Wang, W. Sun, and P. X. Liu, "Adaptive intelligent control of nonaffine nonlinear time-delay systems with dynamic uncertainties," *IEEE Trans. Syst., Man, Cybern. Syst.*, vol. 47, no. 7, pp. 1474–1485, Jul. 2017.

[25] T. O. Andersen, H. C. Pedersen, and M. R. Hansen, "Controlling a conventional LS-pump based on electrically measured LS-pressure," presented at the FPMC, Bath, U.K., 2008.

[26] B. Xu, W. Liu, H. Yang, and M. Cheng, "A new electrohydraulic load sensing control system for hydraulic excavators," in *Proc. 8th Int. Conf. Fluid Power*, Dresden, Germany, 2012, pp. 553–565.

[27] M. Cheng, J. Zhang, B. Xu, R. Ding, and J. Wei, "Decoupling compensation for damping improvement of the electrohydraulic control system with multiple actuators," *IEEE/ASME Trans. Mechatronics*, vol. 23, no. 3, pp. 1383–1392, Jun. 2018.
[28] K. Heybroek, "Saving energy in construction machinery using displacement control hydraulics-concept realization and validation," Ph.D. dissertation, Dept. Manage. Eng., Linköping Univ., Linköping, Sweden, 2008.
[29] M. Axin, B. Eriksson, and P. Krus, "A hybrid of pressure and flow control in mobile hydraulic systems," presented at the 9th Int. Conf. Fluid Power, Aachen, Germany, 2014.
[30] B. Xu, M. Cheng, H. Yang, J. Zhang, and C. Sun, "A hybrid displacement/pressure control scheme for an electrohydraulic flow matching system," *IEEE/ASME Trans. Mechatronics*, vol. 20, no. 6, pp. 2771–2782, Dec. 2015.
[31] X. Zhao, Y. Yin, B. Niu, and X. Zheng, "Stabilization for a class of switched nonlinear systems with novel average dwell time switching by T–S fuzzy modeling," *IEEE Trans. Cybern.*, vol. 46, no. 8, pp. 1952–1957, Aug. 2016.

RUQI DING received the Ph.D. degree in fluid power transmission and control from Zhejiang University, Hangzhou, China, in 2015.

He is currently a Lecturer with the School of Mechatronic Engineering, East China Jiaotong University. His research interests include control systems of mobile machinery, energy saving and motion control of electrohydraulic systems, and mechatronic systems design.

JUNHUI ZHANG received the B.S. and Ph.D. degrees in mechatronics from Zhejiang University, Hangzhou, China, in 2007 and 2012, respectively.

He is currently an Associate Research Fellow with the State Key Laboratory of Fluid Power and Mechatronic Systems, Zhejiang University. His research interests include noise reduction of hydraulic pumps/motors, fluid power components and systems, and mechatronic systems design.

BING XU received the Ph.D. degree in fluid power transmission and control from Zhejiang University, Hangzhou, China, in 2001.

He is currently a Professor and a Doctoral Tutor with the School of Mechanical Engineering, Zhejiang University. He is also the Deputy Director of the State Key Laboratory of Fluid Power and Mechatronic Systems. He has authored or co-authored over 100 journal and conference papers, and 31 patents authorized. His research interests include fluid power components and systems, mechatronics systems design, energy saving, and motion control for mobile machinery. He is a senior member of CMES and CSAA.